Report

Cell Reports

Origin-Dependent Neural Cell Identities in Differentiated Human iPSCs In Vitro and after Transplantation into the Mouse Brain

Graphical Abstract

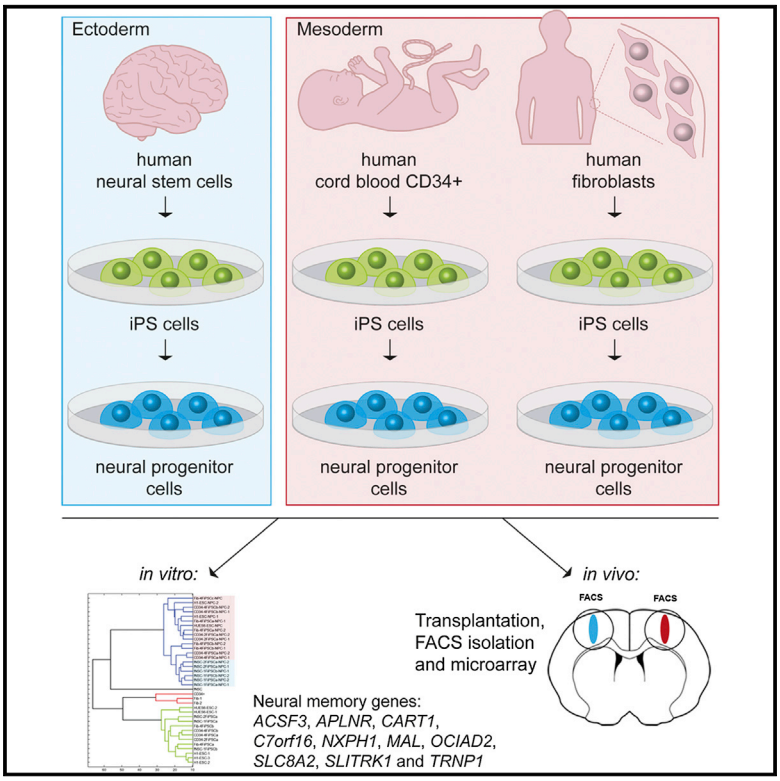

Highlights

Human iPSCs demonstrate origin-dependent expression profiles after neural induction

NPCs from neuroectoderm-derived iPSCs share reprogramming memory with fetal NSCs

Origin-dependent neural cell identities are retained after transplantation

Authors

Gunnar Hargus, Marc Ehrlich, ..., Tanja Kuhlmann, Holm Zaehres

Correspondence

office@mpi-muenster.mpg.de

In Brief

Hargus et al. now compare neural induction of human iPSCs generated from fetal neural stem cells, fibroblasts, or cord blood $CD34^+$ hematopoietic cells. Whole-genome and neural gene-specific transcriptomic analyses reveal a separation of neuroectoderm-derived iPSC-NPCs from mesoderm-derived iPSC-NPCs. They identify "memory genes" that are similarly expressed in fNSCs and neuroectoderm, but not in mesoderm-derived iPSC-NPCs. These neural signatures are retained after transplantation into the murine cortex and correlate with increased survival of neuroectoderm-derived cells.

Accession Numbers

GSE55107

Hargus et al., 2014, Cell Reports 8, 1697–1703
September 25, 2014 ©2014 The Authors
http://dx.doi.org/10.1016/j.celrep.2014.08.014

Cell Reports
Report

Origin-Dependent Neural Cell Identities in Differentiated Human iPSCs In Vitro and after Transplantation into the Mouse Brain

Gunnar Hargus,[1,2,11] Marc Ehrlich,[1,2,11] Marcos J. Araúzo-Bravo,[1,3,4] Kathrin Hemmer,[5,6] Anna-Lena Hallmann,[1,2] Peter Reinhardt,[1] Kee-Pyo Kim,[1] Kenjiro Adachi,[1] Simeon Santourlidis,[7] Foued Ghanjati,[7] Mareike Fauser,[8] Christiana Ossig,[8] Alexander Storch,[8] Jeong Beom Kim,[9] Jens C. Schwamborn,[5,6] Jared Sterneckert,[1] Hans R. Schöler,[1,10,12,*] Tanja Kuhlmann,[2,12] and Holm Zaehres[1,12]

[1]Max Planck Institute for Molecular Biomedicine, 48149 Münster, Germany
[2]Institute of Neuropathology, University Hospital Münster, 48149 Münster, Germany
[3]Group of Computational Biology and Systems Biomedicine, Biodonostia Health Research Institute, 20014 San Sebastián, Spain
[4]IKERBASQUE, Basque Foundation for Science, 48011 Bilbao, Spain
[5]Luxembourg Centre for Systems Biomedicine (LCSB), University of Luxembourg, 4362 Esch-sur-Alzette, Luxembourg
[6]Stem Cell Biology and Regeneration Group, Institute of Cell Biology, ZMBE, Westfälische Wilhelms-University Münster, 48149 Münster, Germany
[7]Institute for Transplantation Diagnostics and Cell Therapeutics, Heinrich-Heine-University, 40225 Düsseldorf, Germany
[8]Division of Neurodegenerative Diseases, Department of Neurology and Center for Regenerative Therapies Dresden (CRTD), University of Technology, 01307 Dresden, Germany
[9]UNIST, Ulsan National Institute of Science and Technology, Ulsan 689-798, South Korea
[10]Faculty of Medicine, University of Münster, 48149 Münster, Germany
[11]Co-first author
[12]Co-senior author
*Correspondence: office@mpi-muenster.mpg.de
http://dx.doi.org/10.1016/j.celrep.2014.08.014

SUMMARY

The differentiation capability of induced pluripotent stem cells (iPSCs) toward certain cell types for disease modeling and drug screening assays might be influenced by their somatic cell of origin. Here, we have compared the neural induction of human iPSCs generated from fetal neural stem cells (fNSCs), dermal fibroblasts, or cord blood CD34$^+$ hematopoietic progenitor cells. Neural progenitor cells (NPCs) and neurons could be generated at similar efficiencies from all iPSCs. Transcriptomics analysis of the whole genome and of neural genes revealed a separation of neuroectoderm-derived iPSC-NPCs from mesoderm-derived iPSC-NPCs. Furthermore, we found genes that were similarly expressed in fNSCs and neuroectoderm, but not in mesoderm-derived iPSC-NPCs. Notably, these neural signatures were retained after transplantation into the cortex of mice and paralleled with increased survival of neuroectoderm-derived cells in vivo. These results indicate distinct origin-dependent neural cell identities in differentiated human iPSCs both in vitro and in vivo.

INTRODUCTION

Induced pluripotent stem cells (iPSCs) carry distinct epigenetic signatures, which, at least in part, are characteristic of their somatic cell of origin (Kim et al., 2010, 2011; Lister et al., 2011; Polo et al., 2010). Low-passage human iPSCs generated from either hematopoietic cells or keratinocytes have a differentiation bias toward their respective starting populations (Kim et al., 2011). These signatures could influence sensitivities of in vitro assays and may require thorough selection of appropriate starting cells prior to iPSC generation. iPSC technology is especially attractive for biomedical research on neurological diseases, as neural cells are not easily accessible from the human brain (Hargus et al., 2014; Reinhardt et al., 2013b; Soldner et al., 2009). However, it is currently not known to what extent neural induction is influenced by the cellular origin of human iPSCs and if any origin-dependent neural cell identities exist, which could influence integrity and maturation of iPSC-derived neural cells in vitro and in vivo.

RESULTS AND DISCUSSION

Robust Differentiation of Human iPSCs into Neural Progenitor Cells In Vitro

To address these questions, we have generated human iPSCs from either brain-derived fetal neural stem cells (fNSC-iPSCs), from mesoderm-derived cord blood CD34$^+$ hematopoietic stem cells (HSCs; CD34$^+$-iPSCs), or from dermal fibroblasts (Fib-iPSCs). All iPSC lines were differentiated into neural progenitor cells (NPCs) according to a protocol we have recently developed (Reinhardt et al., 2013a). These NPCs expressed the neural marker proteins NESTIN, SOX1, SOX2, and FOXA2 and were morphologically indistinguishable between groups (Figure 1A). Quantification revealed comparable differentiation capabilities

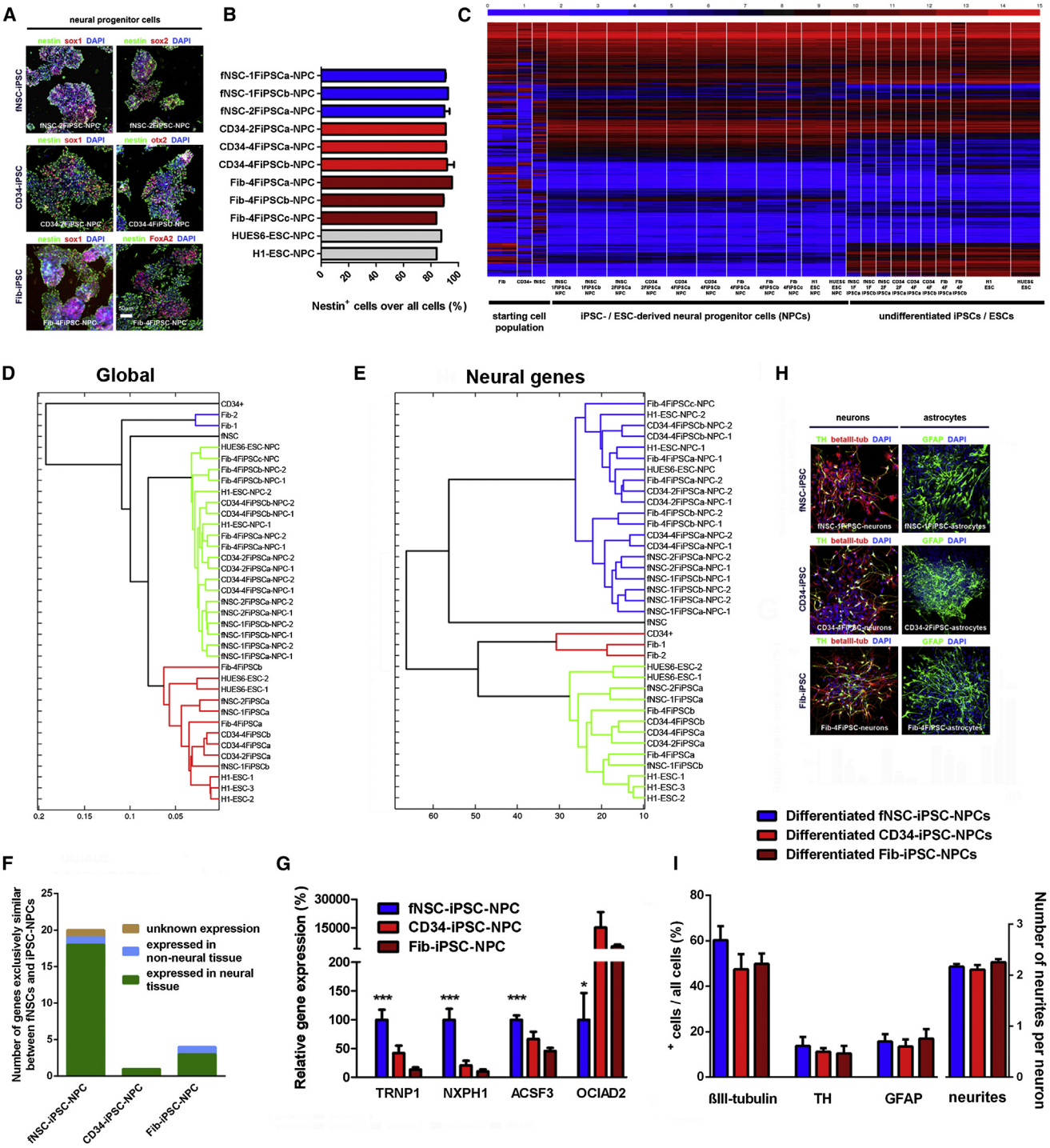

Figure 1. Origin-Dependent Cell Identities in iPSC-Derived Neural Progenitor Cells

Human iPSCs from fetal neural stem cells (fNSCs), CD34$^+$ hematopoietic stem cells (CD34$^+$), and dermal fibroblasts (Fib) were differentiated into neural progenitor cells (NPCs) along with human ESCs.

(A) Immunostainings of NPCs for neural progenitor marker molecules.

(B) Quantification of immunostainings for Nestin.

(C and D) Whole-genome expression profiles of starting cells (fNSCs, CD34, Fib), of undifferentiated iPSCs and ESCs, and of NPCs differentiated from neuroectoderm- and mesoderm-derived iPSCs and from ESCs presented (C) as a heatmap and (D) as hierarchical clusters.

(E) Hierarchical cluster analysis of brain-associated neural genes.

(legend continued on next page)

with about 90% NESTIN$^+$ cells among the different NPC populations (fNSC-iPSC-NPC: 89.1% ± 7.2%; CD34-iPSC-NPC: 89.9% ± 3.9%; Fib-iPSC-NPC: 89.3% ± 4.6%; Figure 1B). This high differentiation efficiency among all groups and the high purity of cultures allowed us to perform whole-genome expression analysis on iPSC-derived neural cells. Thus, expression profiles were collected from several fNSC-iPSC-NPC, CD34-iPSC-NPC, and Fib-iPSC-NPC clones that had been differentiated in parallel and in independent experiments. In addition, we collected expression profiles of the starting cell populations (fNSCs, CD34$^+$ HSCs, and fibroblasts) and of undifferentiated fNSC-iPSCs, CD34-iPSCs, and Fib-iPSCs (Figures 1C and 1D). As reference controls, undifferentiated human embryonic stem cells (ESCs; lines H1 and HUES6) and differentiated ESCs (H1-NPCs and HUES6-NPCs) were also included in the analysis. As expected, the transcriptome analysis demonstrated a clear separation of all NPCs from the starting cells as well as from undifferentiated iPSCs and ESCs (Figures 1C and 1D). Interestingly, among the NPC clones, we discovered that neuroectoderm-derived fNSC-iPSC-NPCs clustered together and separated from mesoderm-derived CD34-iPSC-NPCs and Fib-iPSC-NPCs and from ESC-derived NPCs (Figure 1D). This finding indicated that fNSC-iPSC-NPCs comprised a distinct group among the NPCs, while CD34-iPSC-NPCs and Fib-iPSC-NPCs did not separate as groups from each other in the hierarchical cluster analysis. We would like to note that our iPSCs had been generated with one, two, or four transcription factors, which could have potentially led to differences in gene expression profiles in iPSC-NPCs. However, whole-genome expression analysis revealed reprogramming factor-independent cluster formation of undifferentiated iPSCs with undifferentiated ESCs and separation of lines within the NPC cluster, which was independent of the number of reprogramming factors used for iPSC derivation. We then decided to further characterize neural cell identities of iPSC-derived NPCs in vitro and in vivo.

Identification of Origin-Dependent Cell Identities in Human iPSC-Derived Neural Progenitor Cells In Vitro

The expression of common neural genes such as *NESTIN*, *PTPRZ1*, *POU3F2*, *SOX8*, *SOX2*, *HES5*, and *TUBB3* in NPCs was similar among all NPC groups, demonstrating successful generation of NPCs (Figure S1A). When performing an unbiased expression analysis of 204 brain-associated neural genes obtained from the TiGER database (Liu et al., 2008), we could observe a separation of fNSC-iPSC-NPCs from all other NPCs, as similarly seen in the whole-genome expression analysis (Figure 1E; Figure S1B). Furthermore, we found that all NPC groups clustered closest to fetal brain-derived fNSCs, while undifferentiated iPSCs, CD34$^+$ HSCs, and fibroblasts formed a separate cluster.

These findings provided additional clues to distinct neural characteristics of fNSC-iPSC-NPCs and led us to analyze if fNSC-iPSC-NPCs differed from CD34-iPSC-NPCs and Fib-iPSC-NPCs in regard to their regional identity along the rostrocaudal axis. Indeed, fNSC-iPSC-NPC, in contrast to the mesoderm-derived NPCs, were derived from telencephalic precursor cells, which give rise to cortical and striatal tissue of the developing brain (Kim et al., 2006). Thus, we wondered whether positional identities were erased after derivation and in vitro differentiation of iPSCs. To address this question, we had purposely applied a differentiation protocol to our iPSCs that efficiently generates midbrain/hindbrain precursor cells relevant for disease modeling and drug screening assays in neurodegenerative diseases (Reinhardt et al., 2013a). We determined the expression of *FOXG1*, *LHX2*, *EMX2*, *DLX1*, *DLX2*, *OTX2*, *EN1*, *EN2*, *FOXA2*, *HOXA2*, and *HOXD3* in fNSC-iPSC-NPCs in comparison to CD34-iPSC-NPCs and Fib-iPSC-NPCs (Figure S1C). As expected, fNSCs showed strong expression of the rostral genes *FOXG1*, *LHX2*, *EMX2*, and *DLX1*, while the midbrain-associated genes *EN1*, *EN2*, and *FOXA2* and the hindbrain-associated marker *HOXA2* were virtually not expressed. In contrast, both neuroectoderm- and mesoderm-derived NPCs expressed *EN1*, *EN2*, and *FOXA2* and *HOXA2*, but not *FOXG1*, *LHX2*, and *EMX2*, at high levels, validating the intended differentiation of cells toward caudal domains. However, in contrast to CD34-iPSC-NPCs and Fib-iPSC-NPCs, neuroectoderm-derived fNSC-iPSC-NPCs still showed increased expression of the telencephalic marker *DLX1*, indicating that origin-specific positional identities were vastly, but not entirely, erased in fNSC-iPSC-NPCs (Figures S1C and S1D).

To further characterize neural identities in iPSC-derived NPCs, we performed an unbiased analysis of genes, which were expressed at similar levels in fNSCs and fNSC-iPSC-NPCs but differently expressed in mesodermal NPCs (Figures 1F and 1G; Figure S2D). Since our study included both female and male iPSCs and since an erosion of X chromosome inactivation and thus an erosion of dosage compensation with altered expression of X-linked genes has been described in high-passage iPSCs from female donors (Mekhoubad et al., 2012), which could potentially influence the discovery of origin-dependent signature genes, we decided to exclude any sex chromosome-related genes from this analysis by using only autosomal genes. This approach revealed 20 genes, most of which (18 genes) are expressed in neural tissue, and for half of them (*ACSF3*, *APLNR*, *CART1*, *C7orf16*, *NXPH1*, *MAL*, *OCIAD2*, *SLC8A2*, *SLITRK1*, and *TRNP1*), neural functions such as neural cell adhesion, neural cell migration, or neurite outgrowth have been described (Table S1). Notably, *NXPH1*, *ACSF3*, and *TRNP1* were among the most highly expressed genes in fNSCs and fNSC-iPSC-NPCs, which are expressed in the developing and mature cortex as derivative of the dorsal telencephalon. While *NXPH1*

(F) Number and expression of signature genes similarly expressed in fNSCs and neuroectoderm- or mesoderm-derived NPCs, calculated as specific intersection of differentially regulated genes (DEGs) in fNSCs and NPCs using a fold-change threshold of the absolute value of the replicate mean differences of 4.
(G) Validation of differential expression of signature genes.
(H) Immunostainings of differentiated NPCs for βIII-tubulin, TH, and GFAP.
(I) Quantification of immunostainings for βIII-tubulin, TH, and GFAP and of neurite formation.
Data are presented as mean + SEM. One-way ANOVA with post hoc Tukey test was used as statistical test (*$p < 0.05$; ***$p < 0.001$).

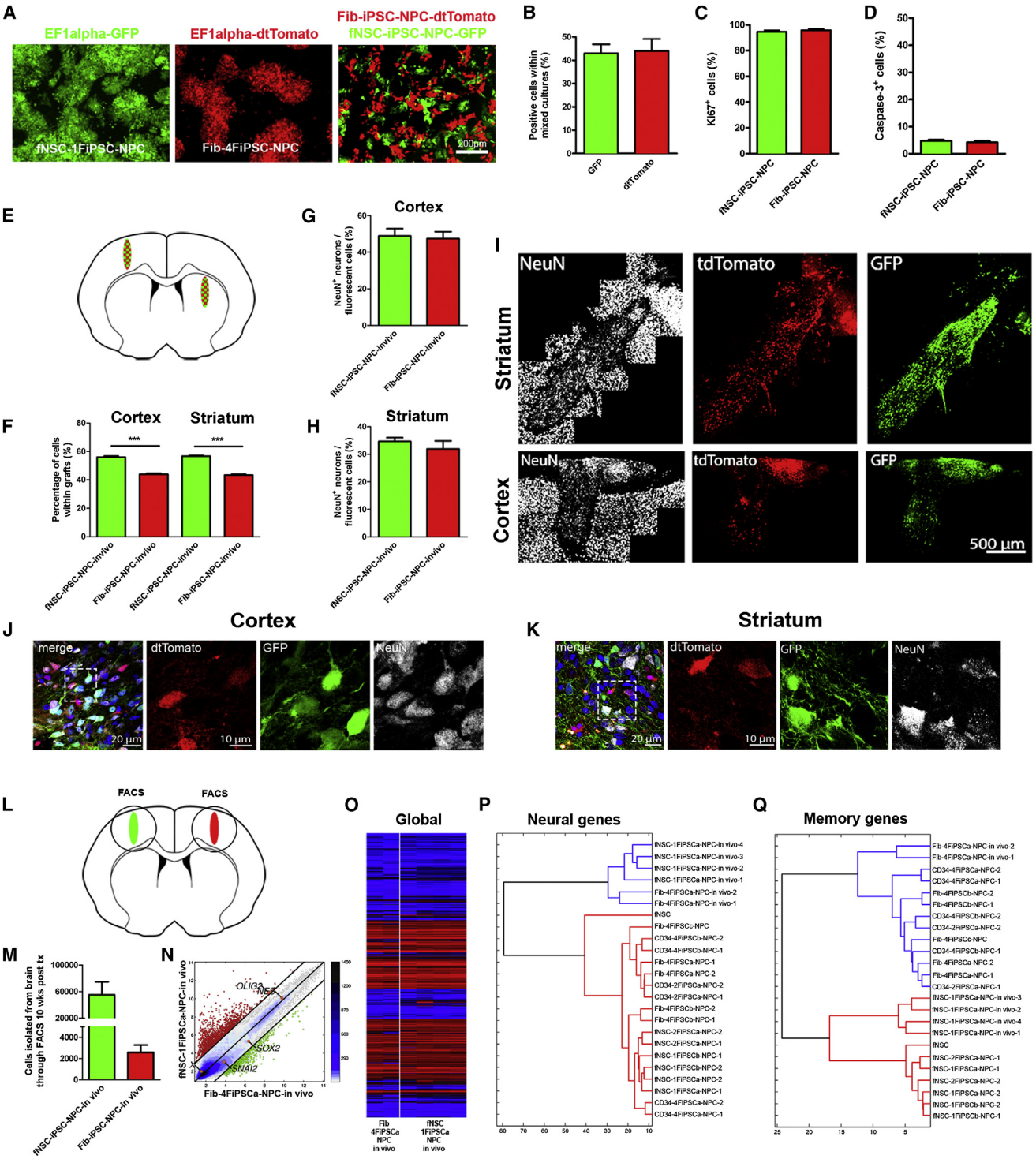

Figure 2. Origin-Dependent Neural Cell Identities in Differentiated iPSCs Are Conserved after Transplantation into the Rodent Brain

(A) Neuroectoderm-derived fNSC-iPSC-NPCs and mesoderm-derived Fib-iPSC-NPCs were transduced with lentiviruses expressing either GFP or dtTomato RFP and cells were mixed at 1:1 ratio prior to transplantation.

(B–D) Nontransplanted NPCs were replated and analysis 1 day after transplantation revealed (B) equal survival rates and similar percentages of (C) proliferating and of (D) apoptotic cells.

(E–K) fNSC-iPSC-NPCs and Fib-iPSC-NPCs were transplanted as mixed cultures into the cortex and striatum of adult mice (n = 4 for each site). (F) Quantification of surviving cells and (G and H) of NeuN$^+$ neurons within grafts 10 weeks after transplantation. (I–K) Immunostainings of cortical and striatal grafts for NeuN demonstrating neuronal maturation of GFP$^+$ and dtTomato$^+$ cells.

(legend continued on next page)

promotes adhesion between dendrites and axons via alpha neurexins in the adult brain (Petrenko et al., 1996), alterations in *ACSF3* have been linked to mental retardation and the development of seizures (Sloan et al., 2011). Interestingly, *TRNP1* has recently been discovered as a DNA-binding protein with essential modulating functions during tangential and radial migration of neuroblasts within the developing cerebral cortex (Stahl et al., 2013), corroborating the identification of distinct origin-dependent identities in fNSC-iPSC-NPCs. Other genes were equally downregulated in fNSCs and fNSC-iPSC-NPCs and included *OCIAD2*, a γ-secretase-activating gene highly expressed in patients with Alzheimer's disease (Han et al., 2014), and *CD70*, a nonneural surface molecule on T and B lymphocytes (Borst et al., 2005). In line with the observation of origin-dependent identities in iPSC-derived NPCs, we identified a significantly smaller number of genes that were exclusively expressed at similar levels in fNSCs and mesodermal NPCs (*LOC339535* in CD34-iPSC-NPCs and *ZP3*, *POMZP3*, *VAV3* and *VGF3* in Fib-iPSC-NPCs) and for which, except for *VGF3*, neural functions have not been described.

To further characterize reprogramming epigenetic memory in neuroectoderm- and mesoderm-derived NPCs, we performed whole-genome promoter methylation analysis on fNSC-iPSC-NPCs, fNSCs, fNSC-iPSCs and CD34-iPSC-NPCs, CD34-HSCs, and CD34-iPSCs using Nimble Gene promoter CpG arrays (Figure S1E). iPSC-derived NPCs formed a distinct group among all cell populations and clearly separated from their iPSCs and their corresponding starting cells ($CD34^+$ HSCs, fNSCs). This finding indicates a significant change of epigenetic marks throughout neural differentiation in both neuroectoderm- and mesoderm-derived NPCs. Interestingly, however, we found shorter distances between fNSC-iPSC-NPCs and fNSCs/fNSC-iPSCs than between CD34-iPSC-NPCs and CD34-HSCs/CD34-iPSCs, indicating smaller extent of epigenetic remodeling and thus a higher number of conserved origin-specific methylation marks in neuroectoderm-derived versus mesoderm-derived NPCs (Figure S1E). In contrast to our transcriptomics data and in contrast to previous methylation studies demonstrating grouping of pluripotent stem cells and separation of these cells from their starting cells (Bock et al., 2011; Lister et al., 2011), fNSCs and fNSC-iPSCs clustered closest to each other, while undifferentiated iPSCs did not cluster with undifferentiated ESCs (Figure S1E). This could be due to the fact that our methylation analysis focused on gene promoter regions, while other groups performed whole genome CpG methylation studies covering both promoter and nonpromoter regions (Bock et al., 2011; Lister et al., 2011; Nazor et al., 2012; Figure S1E). Furthermore, we have recently observed that the reprogramming memory effect can be much stronger at DNA methylation level than at transcriptomics level and have identified DNA sequence methylation patterns specific of reprogramming memory (Luu et al., 2013). We next examined methylation profiles in promoter regions of aforementioned memory genes in neuroectoderm- and mesoderm-derived NPCs to determine whether transcription profiles correlated with distinct epigenetic modifications (Figure S1F). While 12 out of the 20 genetic loci were represented on our Nimble Gene promoter CpG arrays, only 3 out of these 12 genes (*NXPH1*, *MAL*, and *FAM150B*) showed promoter methylation profiles, which correlated with the level of gene expression in iPSC-derived NPCs (Figure S1F). These findings indicated that epigenetic modifications besides promoter DNA methylation, such as histone modifications, may be responsible for the regulation of memory gene expression in iPSC-derived NPCs.

Origin-Dependent Neural Cell Identities Are Retained after Transplantation of Neural Progenitor Cells into the Adult Rodent Brain

So far, these results demonstrated distinct neural characteristics in neuroectoderm- versus mesoderm-derived NPCs and elicited the question if the somatic cell of origin influenced terminal neural differentiation of NPCs into mature neurons and astrocytes. Thus, we first applied differentiation protocols to fNSC-iPSC-NPCs, CD34-iPSC-NPCs, and Fib-iPSC-NPCs and quantified immunostainings for βIII-tubulin, tyrosine hydroxylase (TH), and glial fibrillary acidic protein (GFAP) as well as neurite formation up to 5 weeks after in vitro differentiation (Figures 1H and 1I). This analysis revealed similar neuronal and glial differentiation and maturation capabilities between all NPC groups (Figure 1I). However, this approach did not allow us to analyze whether any neural context-dependent mechanisms influenced neural identities during terminal differentiation of NPCs. Thus, as a proof-of-principle experiment, we decided to transplant neuroectoderm- and mesoderm-derived NPCs into the cortex and striatum of adult mice, which comprise fNSC-derived telencephalic domains within the central nervous system. To visualize cells in vivo, fNSC-iPSC-NPCs and Fib-iPSC-NPCs were labeled with lentiviruses expressing either GFP or dtTomato red fluorescent protein (RFP) prior to transplantation (Figure 2A). We transplanted cells as mixed cell populations consisting of 50% fNSC-iPSC-NPCs and 50% Fib-iPSC-NPCs into the brain, which enabled direct side-by-side analysis of cellular maturation and survival in vivo. In parallel, nontransplanted mixed cell populations were replated in vitro demonstrating equal ratios of GFP^+ and $dtTomato^+$ NPCs (Figure 2B) as well as equivalent numbers of proliferating (Figure 2C) and apoptotic profiles (Figure 2D). All mice contained surviving grafts, which were stained for NeuN and synaptophysin 10 weeks after transplantation (Figures 2E–2K; Figure S2A). In line with our in vitro observations, neuronal differentiation of GFP^+ fNSC-iPSC-NPCs and $dtTomato^+$ Fib-iPSC-NPCs was similar within grafts, indicating cell-autonomous

(L–Q) In an independent experiment, GFP^+ fNSC-iPSC-NPCs and dtTomato+ Fib-iPSC-NPCs were transplanted into the cortex (n = 6) and cells were isolated from brains 10 weeks after transplantation by FACS.
(M) Quantification of isolated fluorescent cells.
(N) Scatterplot comparing gene expression between GFP^+ and $dtTomato^+$ cells.
(O) Heatmap representing global gene expression.
(P and Q) Hierarchical cluster analysis of (P) brain-associated neural genes and of (Q) memory signature genes in in vitro-cultured and transplanted cells.
Data are presented as mean + SEM. Unpaired t test was used as statistical test (**$p < 0.01$; ***$p < 0.001$).

maturation of neuroectoderm- and mesoderm-derived NPCs in vivo (Figures 2G, 2H, 2J, and 2K; Figure S2A). Interestingly, however, we discovered significantly increased numbers of fNSC-iPSC-NPC-derived neural cells within mixed cortical and also mixed striatal grafts (Figure 2F). These findings demonstrated origin-dependent differences in survival of iPSC-derived neurons in the brain and suggested that the neural niche provided a more favorable environment for neuroectodermal versus mesodermal iPSC-derived neurons.

To further analyze if the neural niche and the origin of implanted cells influenced neural identities in vivo, we injected GFP^+ fNSC-iPSC-NPCs and $dtTomato^+$ Fib-iPSC-NPCs in an independent experiment as pure populations into the left and right cortex of adult mice and isolated fluorescent cells from the brain by fluorescence-activated cell sorting (FACS) 10 weeks after transplantation (Figures 2L–2Q). Whole-genome gene expression analysis on isolated cells revealed a separation of the transplanted groups from in vitro-cultured NPCs, reflecting further maturation of progenitor cells into neurons in vivo (Figure 2O; Figure S2B). Concordant with the in vitro data, transplanted NPCs formed a separate cluster when examining expression profiles of brain-associated neural genes, and within the in vivo-group, neuroectoderm-derived neurons clearly separated from mesoderm-derived cells (Figure 2P; Figure S2C). Notably, expression of aforementioned neural signature genes was retained in transplanted fNSC-iPSC-NPCs, which clustered with neuroectoderm-derived fNSCs and cultured fNSC-iPSC-NPCs, while implanted Fib-iPSC-NPCs formed a separate cluster with all mesoderm-derived neural cells (Figure 2Q; Figure S2D).

Our findings demonstrate distinct origin-dependent neural cell identities in human iPSC-derived NPCs in vitro and after transplantation into the adult rodent brain. Interestingly, these differences occurred, although we had used a differentiation protocol, which applies strong guidance cues to undifferentiated iPSCs to efficiently generate homogenous neural cell populations with distinct caudal positional identities (Reinhardt et al., 2013a). It should be noted, though, that both neuroectoderm- and mesoderm-derived NPCs showed robust and comparable differentiation into neurons in vitro and in vivo. We do not argue to use NSCs as starting populations to derive iPSCs (Kim et al., 2009) when intending neurodegenerative disease modeling due to their lack of availability. In fact, we have recently demonstrated that Parkinson's disease patient-derived Fib-iPSC-NPCs, differentiated according to our protocol, comprise suitable cell sources for such purposes (Reinhardt et al., 2013a). However, we would like to raise the point that origin-dependent neural cell identities can exist in human iPSC-derived NPCs.

EXPERIMENTAL PROCEDURES

Derivation and Culture of Neural Progenitor Cells

NPCs were generated and cultured as previously described (Reinhardt et al., 2013a). Briefly, higher-passage pluripotent stem cell colonies (see Supplemental Experimental Procedures for further information) were detached from mouse embryonic fibroblasts 3–4 days after splitting using 2 mg/ml collagenase IV. Pieces of colonies were collected by sedimentation and resuspended in human ESC medium (without FGF2) supplemented with 10 μM SB-431542 (Ascent Scientific), 1 μM dorsomorphin (Tocris), 3 μM CHIR 99021 (Axon Medchem), and 0.5 μM purmorphamine (PMA; Alexis) and subsequently cultured as embryoid bodies (EBs) in Petri dishes. On day 2, medium was changed to N2B27 medium containing the same small-molecule supplements. N2B27 medium consisted of Dulbecco's modified Eagle's medium (DMEM)-F12 (Invitrogen)/Neurobasal (Invitrogen) 50:50 with 1:200 N2 supplement (Invitrogen), 1:100 B27 supplement lacking vitamin A (Invitrogen) with 1% penicillin/streptomycin/glutamine (PAA). On day 4, SB-431542 and dorsomorphin were withdrawn and 150 μM ascorbic acid (AA; Sigma) was added to the medium. On day 6, EBs were triturated into smaller pieces and plated on Matrigel-coated (Matrigel, growth factor reduced, high concentration; BD Biosciences) 12-well plates (Nunc) in NPC expansion medium (N2B27 with CHIR, PMA, and AA). Medium was changed every other day and cells were typically split 1:10–1:15 every 5–6 days. For splitting, cells were digested to single cells for approximately 10 min at 37°C using prewarmed Accutase (PAA). Cells were diluted in DMEM (PAA) and spun down at 1,000 rpm for 5 min. The cell pellet was resuspended in fresh NPC expansion medium and plated on Matrigel-coated cell culture dishes.

Transplantation

GFP-labeled fNSC-iPSC-NPCs or tdTomato-labeled Fib-iPSC-NPCs were trypsinized and resuspended to single cells in DMEM-F12 (Invitrogen) at a density of 50,000 cells per μl. Three microliters of the cell suspension were injected into the right (n = 8) and left (n = 8) hemisphere of the adult mice (n = 8; NOD.CB17-Prkdcscid/NCrHsd mice; Harlan Laboratories) by using a Hamilton 7005KH 5 μl syringe. For intracortical and intrastriatal transplantation of mixed cell populations, cell suspensions were mixed in a ratio of 1:1 prior to transplantation. Independent cell preparations were performed for each mouse. Please see Supplemental Experimental Procedures for more details. All cell transplantation experiments were carried out in accordance with local institutional guidelines under the protocol 87- 51.04.2011.A057, which was approved by Landesamt für Natur, Umwelt und Verbraucherschutz of the state of North Rhine-Westphalia, Germany.

Whole-Genome Expression Analysis

RNA samples for microarray analysis were prepared using RNeasy columns (QIAGEN) with on-column DNA digestion. 300 ng of total RNA per sample was used as the input in the linear amplification protocol (Ambion), which involved the synthesis of T7-linked double-stranded cDNA and 12 hr of in vitro transcription incorporating biotin-labeled nucleotides. Purified and labeled cDNA was then hybridized for 18 hr onto HumanHT-12 v4 expression BeadChips (Illumina) following the manufacturer's instructions. After the recommended washing, the chips were stained with streptavidin-Cy3 (GE Healthcare) and scanned using the iScan reader (Illumina) and the accompanying software. The samples were exclusively hybridized as biological replicates. The RNA samples from in vivo transplanted and FACS-sorted cells were amplified using the TargetAmp 2-Round Biotin-aRNA Amplification Kit 3.0 (Epicenter) from 100 pg to 50 μg.

The bead intensities were mapped to gene information using BeadStudio 3.2 (Illumina), and background correction was performed using the Affymetrix robust multiarray analysis (RMA) background correction model (Irizarry et al., 2003). Variance stabilization was performed using the log2 scaling, and gene expression normalization was calculated with the quantile method implemented in the lumi package of R-Bioconductor. Data postprocessing and graphics were performed with in-house-developed functions in MATLAB (MathWorks). Hierarchical clusters of genes and samples were identified with the one minus the sample correlation metric and the unweighted pair-group method using average (UPGMA) linkage method as previously described (Kim et al., 2009). To identify genes associated with retained reprogramming memory after iPSC differentiation, averages of replicates of respective transcriptomics profiles were calculated before determining differentially expressed genes (DEGs) in iPSC-derived NPCs (Fib-4FiPSCa-NPCs, Fib-4FiPSCb-NPCs, and Fib-4FiPSCc-NPCs; CD34-2FiPSCa-NPCs, CD34-4FiPSCa-NPCs, and CD34-4FiPSCb-NPCs; fNSCs-1FiPSCa-NPCs, fNSCs-1FiPSCb-NPCs, and fNSCs-2FiPSCa-NPCs) in relation to fNSCs using a fold-change threshold of the absolute value of the replicate mean differences of 4 (for each pairwise comparison) and selecting for those genes that were specific, common DEGs in respective intersections (three intersections of DEGs of fNSC-iPSC-NPCs versus fNSCs, intersected with the three

intersections of DEGs of Fib-iPSC-NPCs versus fNSCs, intersected with the three intersections of DEGs of CD34-iPSC-NPCs versus fNSCs). The list of brain-associated neural genes was retrieved from the TiGER database at Wilmer Eye Institute of Johns Hopkins University (Liu et al., 2008).

ACCESSION NUMBERS

The data discussed in this publication have been deposited in NCBI's Gene Expression Omnibus (GEO) and are accessible through GEO Series accession number GSE55107 (http://www.ncbi.nlm.nih.gov/geo/query/acc.cgi?acc=GSE55107).

SUPPLEMENTAL INFORMATION

Supplemental Information includes Supplemental Experimental Procedures, two figures, and two tables and can be found with this article online at http://dx.doi.org/10.1016/j.celrep.2014.08.014.

AUTHOR CONTRIBUTIONS

G.H., M.E., J.S., H.R.S., T.K., and H.Z. developed and designed the study; G.H., M.E., K.H., A.L.H., P.R., K.P.K., K.A., M.F., and C.O. performed experiments; G.H., M.E., M.J.A.B., K.H., A.L.H., J.C.S., A.S., J.S., T.K., and H.Z. analyzed data; M.J.A.B. performed bioinformatics analysis; K.H. performed in vivo transplantations; J.B.K., S.S., and F.G. contributed reagents/materials/analysis tools; and G.H., M.E., H.R.S., T.K., and H.Z. wrote the manuscript. M.J.A.B. and K.H. have contributed equally.

ACKNOWLEDGMENTS

We would like to thank Martina Radstaak, Ingrid Gelker, Elke Hoffmann, Claudia Ortmeier, and Martina Sinn for outstanding technical assistance; Martin Stehling for excellent FACS analysis; and Axel Schambach and Christopher Baum, MHH (Hannover, Germany), for providing the lentiviral SFFV reprogramming vectors. This study was supported by research funding from the IMF at University Hospital Münster (I-HA-111219) to G.H., from a Pélican award from the Fondation du Pélican de Mie et Pierre Hippert-Faber to K.H., by a grant from the National Research Foundation of Korea (NRF) (2010-0020277, 2012M3A9C6049790, 2010-0028684) to J.B.K., from the German Research Foundation (DFG; Emmy Noether Program, SCHW1392/2-1; SFB629 and SPP1356, SCHW1392/4-1), the Schram-Stiftung (T287/21795/2011) and the Fonds National de la Recherche Luxembourg (to J.C.S.), the German Research Foundation (DFG: SFB-TRR128-B7, to T.K.), and the German Federal Ministry of Education and Research (grants BMBF 01GN1008B and BMBF 01GN1006D, to H.R.S. and H.Z.).

Received: January 29, 2014
Revised: May 26, 2014
Accepted: August 7, 2014
Published: September 11, 2014

REFERENCES

Bock, C., Kiskinis, E., Verstappen, G., Gu, H., Boulting, G., Smith, Z.D., Ziller, M., Croft, G.F., Amoroso, M.W., Oakley, D.H., et al. (2011). Reference Maps of human ES and iPS cell variation enable high-throughput characterization of pluripotent cell lines. Cell *144*, 439–452.

Borst, J., Hendriks, J., and Xiao, Y. (2005). CD27 and CD70 in T cell and B cell activation. Curr. Opin. Immunol. *17*, 275–281.

Han, J., Jung, S., Jang, J., Kam, T.I., Choi, H., Kim, B.J., Nah, J., Jo, D.G., Nakagawa, T., Nishimura, M., et al. (2014). OCIAD2 activates gamma-secretase to enhance amyloid beta production by interacting with nicastrin. Cell. Mol. Life Sci. *71*, 2561–2576.

Hargus, G., Ehrlich, M., Hallmann, A.L., and Kuhlmann, T. (2014). Human stem cell models of neurodegeneration: a novel approach to study mechanisms of disease development. Acta Neuropathol. *127*, 151–173.

Irizarry, R.A., Bolstad, B.M., Collin, F., Cope, L.M., Hobbs, B., and Speed, T.P. (2003). Summaries of Affymetrix GeneChip probe level data. Nucleic Acids Res. *31*, e15.

Kim, H.T., Kim, I.S., Lee, I.S., Lee, J.P., Snyder, E.Y., and Park, K.I. (2006). Human neurospheres derived from the fetal central nervous system are regionally and temporally specified but are not committed. Exp. Neurol. *199*, 222–235.

Kim, J.B., Greber, B., Araúzo-Bravo, M.J., Meyer, J., Park, K.I., Zaehres, H., and Schöler, H.R. (2009). Direct reprogramming of human neural stem cells by OCT4. Nature *461*, 649–653.

Kim, K., Doi, A., Wen, B., Ng, K., Zhao, R., Cahan, P., Kim, J., Aryee, M.J., Ji, H., Ehrlich, L.I., et al. (2010). Epigenetic memory in induced pluripotent stem cells. Nature *467*, 285–290.

Kim, K., Zhao, R., Doi, A., Ng, K., Unternaehrer, J., Cahan, P., Huo, H., Loh, Y.H., Aryee, M.J., Lensch, M.W., et al. (2011). Donor cell type can influence the epigenome and differentiation potential of human induced pluripotent stem cells. Nat. Biotechnol. *29*, 1117–1119.

Lister, R., Pelizzola, M., Kida, Y.S., Hawkins, R.D., Nery, J.R., Hon, G., Antosiewicz-Bourget, J., O'Malley, R., Castanon, R., Klugman, S., et al. (2011). Hotspots of aberrant epigenomic reprogramming in human induced pluripotent stem cells. Nature *471*, 68–73.

Liu, X., Yu, X., Zack, D.J., Zhu, H., and Qian, J. (2008). TiGER: a database for tissue-specific gene expression and regulation. BMC Bioinformatics *9*, 271.

Luu, P.L., Schöler, H.R., and Araúzo-Bravo, M.J. (2013). Disclosing the crosstalk among DNA methylation, transcription factors, and histone marks in human pluripotent cells through discovery of DNA methylation motifs. Genome Res. *23*, 2013–2029.

Mekhoubad, S., Bock, C., de Boer, A.S., Kiskinis, E., Meissner, A., and Eggan, K. (2012). Erosion of dosage compensation impacts human iPSC disease modeling. Cell Stem Cell *10*, 595–609.

Nazor, K.L., Altun, G., Lynch, C., Tran, H., Harness, J.V., Slavin, I., Garitaonandia, I., Müller, F.J., Wang, Y.C., Boscolo, F.S., et al. (2012). Recurrent variations in DNA methylation in human pluripotent stem cells and their differentiated derivatives. Cell Stem Cell *10*, 620–634.

Petrenko, A.G., Ullrich, B., Missler, M., Krasnoperov, V., Rosahl, T.W., and Südhof, T.C. (1996). Structure and evolution of neurexophilin. J. Neurosci. *16*, 4360–4369.

Polo, J.M., Liu, S., Figueroa, M.E., Kulalert, W., Eminli, S., Tan, K.Y., Apostolou, E., Stadtfeld, M., Li, Y., Shioda, T., et al. (2010). Cell type of origin influences the molecular and functional properties of mouse induced pluripotent stem cells. Nat. Biotechnol. *28*, 848–855.

Reinhardt, P., Glatza, M., Hemmer, K., Tsytsyura, Y., Thiel, C.S., Höing, S., Moritz, S., Parga, J.A., Wagner, L., Bruder, J.M., et al. (2013a). Derivation and expansion using only small molecules of human neural progenitors for neurodegenerative disease modeling. PLoS ONE *8*, e59252.

Reinhardt, P., Schmid, B., Burbulla, L.F., Schöndorf, D.C., Wagner, L., Glatza, M., Höing, S., Hargus, G., Heck, S.A., Dhingra, A., et al. (2013b). Genetic correction of a LRRK2 mutation in human iPSCs links parkinsonian neurodegeneration to ERK-dependent changes in gene expression. Cell Stem Cell *12*, 354–367.

Sloan, J.L., Johnston, J.J., Manoli, I., Chandler, R.J., Krause, C., Carrillo-Carrasco, N., Chandrasekaran, S.D., Sysol, J.R., O'Brien, K., Hauser, N.S., et al.; NIH Intramural Sequencing Center Group (2011). Exome sequencing identifies ACSF3 as a cause of combined malonic and methylmalonic aciduria. Nat. Genet. *43*, 883–886.

Soldner, F., Hockemeyer, D., Beard, C., Gao, Q., Bell, G.W., Cook, E.G., Hargus, G., Blak, A., Cooper, O., Mitalipova, M., et al. (2009). Parkinson's disease patient-derived induced pluripotent stem cells free of viral reprogramming factors. Cell *136*, 964–977.

Stahl, R., Walcher, T., De Juan Romero, C., Pilz, G.A., Cappello, S., Irmler, M., Sanz-Aquela, J.M., Beckers, J., Blum, R., Borrell, V., and Götz, M. (2013). Trnp1 regulates expansion and folding of the mammalian cerebral cortex by control of radial glial fate. Cell *153*, 535–549.